Chapter 1
Gravitational Collapse and Disk Formation in Magnetized Cores

Susana Lizano and Daniele Galli

Abstract We discuss the effects of the magnetic field observed in molecular clouds on the process of star formation, concentrating on the phase of gravitational collapse of low-mass dense cores, cradles of sunlike stars. We summarize recent analytic work and numerical simulations showing that a substantial level of magnetic field diffusion at high densities has to occur in order to form rotationally supported disks. Furthermore, newly formed accretion disks are threaded by the magnetic field dragged from the parent core during the gravitational collapse. These disks are expected to rotate with a sub-Keplerian speed because they are partially supported by magnetic tension against the gravity of the central star. We discuss how sub-Keplerian rotation makes it difficult to eject disk winds and accelerates the process of planet migration. Moreover, magnetic fields modify the Toomre criterion for gravitational instability via two opposing effects: magnetic tension and pressure increase the disk local stability, but sub-Keplerian rotation makes the disk more unstable. In general, magnetized disks are more stable than their nonmagnetic counterparts; thus, they can be more massive and less prone to the formation of giant planets by gravitational instability.

1.1 Introduction

The goal of this review is to summarize recent theoretical work addressing the role of magnetic fields in the process of star formation, and, in particular, on the for-

Susana Lizano

Centro de Radioastronomía y Astrofísica, UNAM, Apartado Postal 3-72, 58089 Morelia, Michoacán, México
e-mail: s.lizano@crya.unam.mx

Daniele Galli

INAF-Osservatorio Astrofisico di Arcetri, Largo E. Fermi 5, I-50125, Firenze, Italy
e-mail: galli@arcetri.astro.it

mation of circumstellar disks. In fact, the interstellar magnetic field dragged in the star plus disk system by the collapse of the parent cloud affects in the first place the process of disk formation itself (Section 1.3.1), but also provides a natural mechanism for disk viscosity and resistivity via the MRI instability (Section 1.4.1), affects the rotation curve of the disk (Section 1.4.2), its stability properties (Section 1.4.3), and the migration of planets (Section 1.4.4). Unfortunately, the detection of magnetic fields in circumstellar disks is still an observational challenge (Section 1.3.2). For recent comprehensive reviews see, e.g., König & Salmeron (2011) for the role of magnetic fields in the process of disk formation, and Armitage (2011) for the evolution of protoplanetary disks.

1.2 Magnetic Fields in Molecular Clouds

Theoretical considerations (Chandrasekhar & Fermi 1953, Mestel & Spitzer 1956) show that a cloud of mass M enclosing a magnetic flux Φ can be supported by the magnetic field against its self-gravity provided its non-dimensional mass-to-flux ratio λ expressed in units of $(2\pi G^{1/2})^{-1}$ where G is the gravitational constant, is less than unity,

$$\lambda \equiv 2\pi G^{1/2} \left(\frac{M}{\Phi} \right) < 1. \tag{1.1}$$

Subcritical clouds with $\lambda < 1$ evolve on a timescale that characterizes the diffusion of the magnetic field (e.g., Nakano 1979). On the other hand, supercritical clouds with $\lambda > 1$ cannot be supported by the magnetic field alone, even if the field were perfectly frozen in the gas. These clouds would collapse on a magnetically diluted free-fall timescale.

A large number of measurements of the intensity of the magnetic field has been obtained for different ISM conditions with various techniques (see e.g. Crutcher 2012 and the chapter by Crutcher, this volume). The available measurements of magnetic field strength in molecular clouds support the conclusion that on average, clouds are close to the critical value $\lambda \approx 1$. OH Zeeman measurements at cloud densities $\sim 10^3$ cm^{-3} give mean mass-to-flux ratios $\lambda \sim 2$–3 (Crutcher & Troland 2008). In dense cores, the mean value of the mass-to-flux ratio from CN Zeeman observations is $\lambda \sim 2$. Nevertheless, due to uncertainties in the measurement of the gas column densities of a factor ~ 2, a possible range of mass-to-flux ratios is $\lambda \sim 1$–4 (Falgarone et al. 2008). As we discuss below, these observed magnetic fields are dynamically important for the cloud evolution and gravitational collapse to form stars. In fact, these fields are well ordered on the large scales of molecular clouds (e.g., Goldsmith et al. 2008).

Thanks to the presence in the ISM of aspherical dust grains aligned with the field, polarization maps of the thermal emission of molecular clouds at submillimeter wavelengths have made possible to determine the field geometry and the relative importance of the ordered and turbulent components of the magnetic field. At

the core scales, recent SMA maps of polarized dust continuum emission show the hourglass morphology expected for a magnetically controlled collapse rather than a disordered field dominated by important levels of turbulent motions (e.g., Girart et al. 2006, 2009; Gonçalves et al. 2008, Tang et al. 2009). Moreover, the statistical analysis of submillimeter polarization maps based on the dispersion function method, shows that the ratio of the rms turbulent component of the magnetic field to the mean value is of the order of 0.1–0.5 (Hildebrand et al. 2009; Houde et al. 2009). Thus, turbulent motions do not dominate the large scale well ordered magnetic field.

As a first approximation, the magnetic field in molecular clouds can be considered frozen to the gas. Even though the gas is is lightly ionized, with an ionization fraction $\sim 10^{-8}$–10^{-7} (see e.g. Caselli et al. 1998), collisions between charged particles and neutrals efficiently transmit the Lorentz force to the largely neutral gas. In these conditions, the relevant mechanism of field diffusion is ambipolar diffusion (hereafter AD), originally proposed by Mestel & Spitzer (1956), a process by which the fluid of charged particles attached to the magnetic field can slowly drift with respect to the fluid of neutral particles (see chapter by Zweibel in this volume). The field is then left behind with respect to the neutral gas and the mass-to-flux ratio increases as the cloud condenses under the influence of its self-gravity. Thus, an initially magnetically subcritical region of mass sufficiently high for its self-gravity to overcome the support provided by thermal pressure and turbulent motions, evolves under this process toward a centrally condensed core with supercritical mass-to-flux ratio, $\lambda \geq 1$ that eventually collapses and fragments (e.g., Lizano & Shu 1989; Tomisaka et al. 1990). These authors showed that, for typical conditions of molecular clouds (densities $\sim 10^3$ cm^{-3}, magnetic fields $B \sim 30\ \mu$G), the AD timescale for core formation was a few $\times 10^6$ yr. Once the dense cores are formed, with densities of $\sim 3 \times 10^4$ cm^{-3}, they quickly evolve toward the stage of gravitational collapse in a few $\times 10^5$ yr, of the order of the free-fall timescale. The mass-to-flux ratio increases little in this condensation process of core formation, thus, the major phase of flux loss occurs at higher densities. At core densities, also Ohmic losses are far too small to significantly reduce the magnetic field strength. For example, for an ionization fraction $\sim 10^{-8}$ and density $\sim 10^5$ cm^{-3}, the Ohmic dissipation time of a magnetic field extending on a length scale of ~ 0.1 pc is of the order of 10^{15} yr. In contrast, at higher density, $n \sim 10^{11}$ cm^{-3}, characteristic of circumstellar disk formation, the field can be effectively removed from the system by processes like Ohmic diffusion and the Hall effect (see, e.g. Pinto et al. 2008; Pinto & Galli 2008). At some point in the star formation process magnetic field removal is necessary to prevent the formation of stars with MG fields, as would be the case under field freezing conditions. This has been called the "magnetic flux" problem by Mestel & Spitzer (1956). Current observations show that at the surface of young stars the fields have magnitudes of kG (e.g., Johns-Krull et al. 1999, 2004), they are likely to be generated by dynamo action, rather than being fossil fields.

It has been under debate whether the formation and evolution of the dense cores is controlled by magnetic fields as discussed above (e.g., Mouschovias & Ciolek 1999; Adams & Shu 2007; Nakamura & Li 2008) or by gravo-turbulent fragmentation driven by supersonic turbulence (e.g., Padoan et al. 2001; Klessen et

al. 2005; Vázquez-Semadeni et al. 2005), or by hierarchical gravitational collapse of a cloud as a whole (e.g., Ballesteros-Paredes et al. 2011a,b and chapter by Vázquez-Semadeni in this volume). We favor the first process because the large scale magnetic fields dominate over their turbulent components and they are strong enough to contribute to the support of a cloud core against its self-gravity if λ is of order unity. Furthermore, as we will discuss below, these fields influence the dynamics of the gravitational collapse and they are difficult to get rid of.

The process of gravitational collapse therefore separates logically into two phases: (*a*) how cloud cores that were initially sub-critical evolve to a state of being super-critical, and (*b*) how cloud cores of both low and high mass that are super-critical subsequently gravitationally collapse and possibly fragment once they pass beyond the threshold of stability. In this chapter we will focus on the second problem, the phase of gravitational collapse of a super-critical magnetized rotating core to form a star-disk system.

1.3 Gravitational Collapse of Magnetized Cores

1.3.1 Catastrophic Magnetic Braking and Disk Formation

Recently, several studies have addressed the gravitational collapse of a magnetized rotating cloud core to form a protostar plus disk system. These studies have considered the ideal magnetohydrodynamic (MHD) regime where the magnetic flux is frozen to the fluid, and the non-ideal MHD regime where several diffusive processes are taken into account. In particular, in their seminal work, Allen et al. (2003) followed the ideal MHD collapse of a core threaded by a large scale poloidal field, taking as an initial state a singular isothermal uniformly rotating toroid (Li & Shu 1996). They found a pseudo-disk predicted by Galli & Shu (1993a,b), a non-equilibrium flattened structure formed around the star by the tendency of the gas to flow along field lines and by the pinching Lorentz force resulting from the bending of the field dragged to the central star. These simulations also produced the slow outflows (with velocities of few km s^{-1}) found in previous numerical studies (e.g, Tomisaka 2002). Nevertheless, the simulations did not show the formation of a rotationally supported disk (RSD). Allen et al. argued that RSDs do not form in the ideal MHD regime because the enhanced strength and increased lever arm of the magnetic field dragged into the center of collapse results in a very efficient transfer of angular momentum from the accretion region to the cloud envelope. Subsequent numerical simulations confirmed that RSDs naturally form if $B = 0$ but do not form in strongly magnetized clouds (e.g., Price & Bate 2007, Fromang et al. 2006, Duffin & Pudritz 2009). In fact, the process of magnetic braking was known to provide a way to remove the cloud angular momentum and to allow the formation of disks and binary stars (e.g., Mouschovias & Paleologou 1980). However, the braking found in

these simulations of the gravitational collapse phase was too efficient and prevented altogether the formation of a disk.

Galli et al. (2006) studied the self-similar collapse of an axisymmetric isothermal magnetized rotating cloud in the ideal MHD regime and found an analytic solution that asymptotically approaches free fall onto a central mass point, with an angular distribution that depends on the mass loading of magnetic field lines. They found that, independent on the details of the starting state, the magnetic field acquires a split-monopole configuration where the magnetic field is almost radial and directed in opposite directions above and below the mid plane. In this configuration the radial magnetic field strength increases as the inverse square of the distance r from the origin,

$$|B_r| = \phi_* \frac{c_s^3 t}{G^{1/2} r^2},\tag{1.2}$$

where ϕ_* is the non-dimensional magnetic flux trapped in the central source, c_s is the sound speed and t is the time since the onset of collapse. This strong field produces a very efficient magnetic braking that prevents the formation of a RSD. The azimuthal velocity of the infalling gas decreases to zero at the center as $u_\varphi \propto -jr^{1/2}$, where j is the specific angular momentum of the gas in the envelope. Thus, the gas spirals into the star with velocity approaching free-fall, $u_r \propto r^{-1/2}$. The negative sign in the azimuthal velocity indicates that the magnetic braking is so efficient as to enforce counter rotation in the infalling gas, very close to the protostar. This counter rotation of the innermost parts of the accretion flow has also been found in numerical simulations (Mellon & Li 2009; Kransnopolsky et al. 2010). The azimuthal component of the magnetic field decreases as $B_\varphi \propto r^{-1}$ that increases with decreasing radius more slowly than the poloidal component given by Equation 1.2. Thus, the winding of the field goes to zero near the protostar. Figure 1.1 illustrates the velocity field of the accretion flow in the equatorial plane of a magnetized rotating cloud. In this figure the inner solution of Galli et al. (2006) has been matched *ad hoc* to the outer rotating flow. The flow shows counter rotation at the center, before the gas falls onto the star.

Summarizing, in the absence of magnetic torques, the angular momentum of infalling fluid elements is conserved and a RSD is formed inside a radius r_d, where the azimuthal velocity, increasing as r^{-1}, becomes equal to the Keplerian velocity around the protostar, increasing like $r^{-1/2}$. Instead, when magnetic braking dominates over angular momentum conservation, the azimuthal velocity goes to zero at small radii, and no RSD is formed. Galli et al. named this process "catastrophic magnetic braking" and concluded that the dissipation of dynamically important levels of magnetic field is a fundamental requisite for the formation of protoplanetary disks around young stars.

Several numerical simulations addressed the question of determining the maximum level of magnetization required to allow disk formation under field-freezing conditions. These studies have found that disk formation is possible only for clouds with mass-to-flux ratios $\lambda > 10$—80 (Mellon & Li 2008; Hennebelle & Fromang 2008; Seifried et al. 2011), or $\lambda > 3$ for misaligned magnetic and rotation axis (Hennebelle & Ciardi 2009; Joos et al. 2012). Nevertheless, misalignment alone is
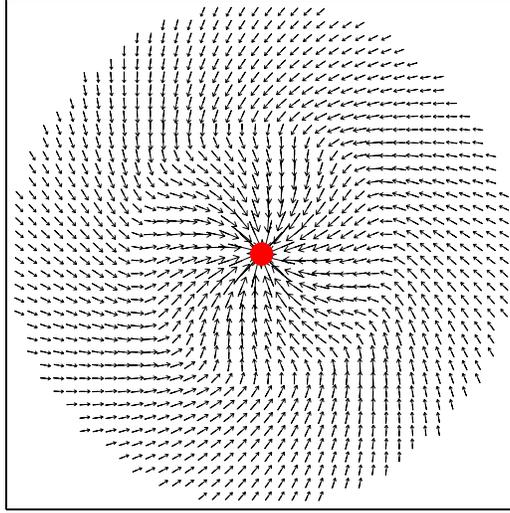
Fig. 1.1 Illustration of the velocity field of the accretion flow in the equatorial plane of a magnetized rotating cloud. In this figure the inner solution of Galli et al. (2006) has been matched to the outer rotating flow. Because the azimuthal velocity decreases as $u_\varphi \propto -jr^{1/2}$ for $r \to 0$, where j is the gas specific angular momentum at large distance, no rotationally supported disk is formed. The flow shows a counter rotation at the center, before the gas falls into the star. The magnetic field lines coincide with the streamlines outlined by the arrows.

unlikely to solve the problem of catastrophic magnetic braking at least for cores with $\lambda \approx 2$ (Li et al. 2013). Krumholz et al. (2013) recently proposed that a combination of misalignment *and* weakness of the magnetic field may lead to the formation of disks in agreement with the observed fractions around embedded protostars. However, since the mass-to-flux ratio in molecular clouds is $\lambda \sim 1$–4 as discussed in §1.1, it is clear the constraint of ideal MHD must be relaxed at some point to allow the formation of rotationally (rather than magnetically) supported disks.

Shu et al. (2006) solved analytically the problem of gravitational collapse of a magnetized cloud with a uniform resistivity η, in the kinematic approximation, i.e. neglecting the back reaction of the magnetic field on the motion of the gas. Under this simplifying assumption, dissipation of the magnetic field occurs inside a sphere with radius r_{Ohm}, that is inversely proportional to the instantaneous stellar mass $M_*(t)$, and proportional to the square of the electrical resistivity η, which may include Ohmic dissipation and AD:

$$r_{\mathrm{Ohm}} \equiv \frac{\eta^2}{2GM_*} \approx 10 \left(\frac{\eta}{10^{20}\ \mathrm{cm^2\ s^{-1}}} \right)^2 \left(\frac{M_*}{M_\odot} \right)^{-1}\ \mathrm{AU}. \tag{1.3}$$

Shu et al. showed that for values of $\eta \sim 10^{20}$ cm^2 s^{-1}, the strength of the uniform magnetic field around the accreting protostar is $B \sim 1$ G, of the order of the measured values in meteorites. This anomalous resistivity is a few orders of magnitude larger than the microscopic resistivity found by Nakano et al. (2002) for the densities and ionization conditions of pseudo-disks (see also Li et al. 2011). Kransnopolsky et al. (2010) performed axisymmetric numerical simulations of resistive MHD relaxing the kinematic approximation, and found that lower values of the resistivity $\eta \sim 10^{19}$ cm^2 s^{-1} were enough to allow the formation of RSDs. Shu et al. also pointed out that the luminosity resulting from the Ohmic dissipation of the electric current can be very large,

$$L_{\text{Ohm}} \sim 300 \lambda^{-2} \left(\frac{M_*}{M_\odot} \right)^5 \left(\frac{\eta}{10^{20}\,\text{cm}^2\,\text{s}^{-1}} \right)^{-5} L_\odot. \qquad (1.4)$$

In fact, the resistivity cannot be much smaller than the values quoted above, without violating the constraints on the observed protostellar luminosity.

Krasnopolsky & Königl (2002) and Braiding & Wardle (2011) studied self-similar 1-D models of the gravitational collapse of a flattened rotating, magnetized cloud. Krasnopolsky & Königl found that magnetic flux piles up at the so-called "AD shock" increasing the efficiency of magnetic braking. Braiding & Wardle included also the Hall effect and found that RSDs could form for appropriate values of the Hall coefficient and orientation of the magnetic field, since the Hall diffusion is not invariant under field reversal. However, in these self-similar models the diffusion coefficients scale as $c_s^2 t$. Thus, at typical times, $t \sim 10^{4-5}$ yr, and for $c_s \sim 0.2$ km s^{-1},
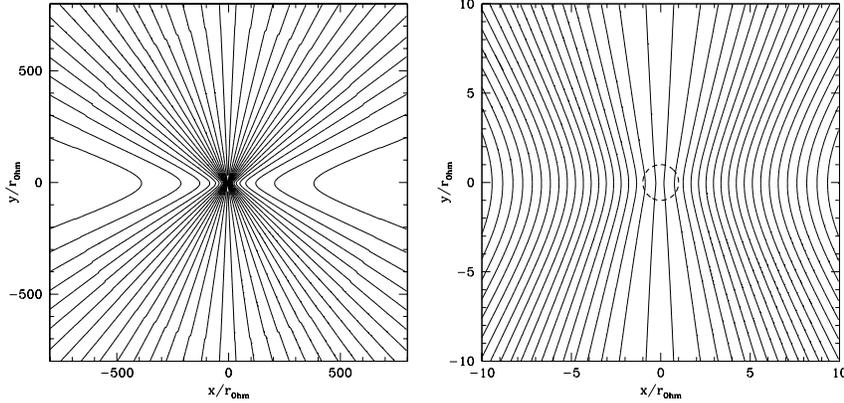

Fig. 1.2 Magnetic field configuration in the meridional plane for magnetized cloud collapse with uniform resistivity. Distances are measured in units of the Ohm radius r_{Ohm}. The left panel shows the field lines at large distance from the central source, inside the region of radius $\leq 500\,r_{\text{Ohm}}$. The right panel shows the field lines inside a region of radius $\leq 10\,r_{\text{Ohm}}$ from the center. The dashed circle has a radius equal to r_{Ohm} (Figure from Galli et al. 2009).

they have values $\sim 10^{20}$–10^{21} cm^2 s^{-1}, larger than the expected microscopic values, in agreement with Shu et al. (2006).

In recent years, several MHD simulations have been carried out that include different non-ideal processes: Ohmic dissipation, AD, and the Hall effect (see, e.g., Mellon & Li 2009; Krasnopolsky et al. 2010, 2011; Li et al. 2011). These simulations find that, for realistic levels of cloud magnetization and cosmic ionization rates, flux redistribution by AD is not enough to allow the formation of a RSD; and, as discussed above, in some cases, AD can even enhance the magnetic braking. They also require anomalous Ohmic resistivity to form RSDs, and find that the Hall effect can spin up the gas even in the case of an initially non-rotating cloud, although the disks formed this way are sub-Keplerian. These authors conclude that the combined effects of these diffusion mechanisms may weaken the magnetic braking enough to form RSDs.

Machida et al. (2011) performed 3-D resistive MHD simulations of the collapse of strongly magnetized clouds ($\lambda \approx$ 1–3). Keeping the magnetic field anchored in the cloud's envelope, they found that the efficiency of magnetic braking depends on disk/envelope mass ratio: magnetic braking is very efficient during the main accretion phase when the envelope is much more massive than the forming disk and the disk radius remains $\sim$10 AU or less; magnetic braking then becomes largely ineffective when most of the envelope mass has been accreted by the star/disk system. As a consequence, the disk expands to a radius of $\sim$ 100 AU during the late accretion phase, when the residual envelope mass is reduced to $\sim$ 70–80% of the initial value (for a low-mass core). This work suggests that Class 0 sources would have small disks, while older sources would develop the observed hundred AU disks, a prediction that could be tested by the new generation interferometer ALMA. In contrast with all other ideal MHD simulations, Machida et al. also find the formation of a RSD in the ideal MHD regime. A convergence study is necessary to asses the possible influence of numerical diffusion in this result. Also Dapp & Basu (2010) and Dapp et al. (2012) find that Ohmic dissipation with normal microscopic values is effective at high densities and RSDs can form. Nevertheless, their simulations address very early times, when the disk has a size of only several stellar radii around a protostar with mass $\sim 10^{-2} M_\odot$. In particular, their simulations are stopped when the expansion wave is only 15 AU away. This is too early in the protostellar evolution process to determine the possibility that the disk can survive through all the accretion phase.

Another diffusion mechanism that has been proposed recently is the reconnection diffusion of the magnetic field in a turbulent medium (Lazarian & Vishniac 1999). In particular, Santos-Lima et al. (2012) performed collapse simulations to study this process and find a disk that is rotationally supported at radii between $\sim$ 65–120 AU. Seifried et al. (2012) also included turbulence in ideal MHD simulations and claimed that this effect alone can lead to the formation of RSDs, without the requirement of magnetic flux loss. Nevertheless, these authors acknowledge a very high numerical diffusion in the region of disk formation that, as discussed above, probably accounts for the field dissipation and the weakening of the magnetic braking. Furthermore, Santos-Lima et al. (2013) argued that their apparent constant mass-

to-flux ratio is due to their averaging over a large volume which can mask the flux loss. On the other hand, it should also be kept in mind that observations indicate that dense cores are quiescent with the presence of only subsonic turbulence (e.g., Pineda et al. 2010). Therefore, any proposed mechanism of field diffusion should be able to work efficiently in conditions of weak turbulence. Also, since the small scales of the actual process of field reconnection cannot be resolved in the numerical simulations, the authors rely on numerical diffusion to mimic this physical process. We thus consider that further tests and, possibly, semi-analytic studies are necessary to determine the efficiency of reconnection diffusion and the physical properties of disks produced by this mechanism.

Finally, it is interesting to notice that several numerical simulations have found that the efficient braking and extra support provided by magnetic fields inhibit cloud fragmentation (e.g., Hosking & Whitworth 2004; Hennebelle & Teyssier 2008; Duffin & Pudritz 2009; Commerçon et al. 2010, 2011). Also, the MHD numerical simulations that have been carried out to study the problem of magnetic field diffusion assume in general an isothermal equation of state and do not compute the energy released by field dissipation. This power could be appreciable (see Equation 1.4), and would be available to heat the gas and the dust, accelerate particles, and thus, increase the ionization. It would be important to include these effects in a self-consistent way in current models (e.g., Padovani et al. 2009; Glassgold et al. 2012).

In conclusion, how observed RSDs are formed around protostars is still an open question. The answer is probably a combination of diffusive processes at high densities plus the dissipation of the core envelope where the angular momentum is deposited by magnetic braking.

1.3.2 Measurements of Mass-to-Flux Ratios in Protostellar Disks

It is possible to estimate the values of the mass-to-flux ratio of some star-disk systems and compare them to the measured values in molecular cloud cores. This comparison provides an observational constraint on the amount of magnetic flux dragged by the disk. At very large disk radii, magnetic field strengths of the order of a few mG have been measured by Zeeman splitting in OH maser rings associated to high-mass protostars (see Table 1.1 for references). These ringlike configurations have radii of order 10^3 AU, are elongated in the direction perpendicular to the outflow, and are usually characterized by a linear velocity gradient, suggestive of rotation or accelerated expansion (see Cesaroni et al. 2007 for a review). In general, these observations suggest that, at these radii, the field is mostly poloidal, although the presence of reversals might indicate the presence of a toroidal component probably generated by rotation. Assuming that these measurements actually probe a disk field and that it is possible to estimate the system mass from the observed kinematics of the maser rings, one can obtain the mass-to-flux ratio of the system. If the vertical component of the field B_z scales with radius like $B_z(\varpi) \propto \varpi^{-(1+\alpha)}$, with $\alpha \approx 3/8$ (Shu et al. 2007; see also discussion in §1.3), most of the disk magnetic flux Φ_d is

Table 1.1 Estimates of the mass-to-flux ratio λ_{sys} in circumstellar disks around massive stars from OH Zeeman measurements.

source	u_φ (km s^{-1})	B_z (mG)	ϖ (10^3 AU)	λ_{sys}	reference
W57N	6	7	3	2.7	Hutawarakorn et al. (2002)
IRAS20126	3	11	0.85	1.5	Edris et al. (2007)
G35.2-0.74N	5	5	2.6	3.1	Hutawarakorn & Cohen (1999)
AFGL2591	5	4	0.75–1.5	6.7-13	Hutawarakorn & Cohen (2005)

at large radii, $\Phi_d = 2/(1-\alpha)B_z(\varpi)\varpi^2$. The enclosed mass of disk plus star can be estimated from the observed rotation, such that $G(M_d + M_*) \approx u_\varphi^2(\varpi)\varpi$. With these assumptions, the mass-to-flux ratio of the system is

$$\lambda_{sys} = \frac{2\pi G^{1/2}(M_* + M_d)}{\Phi_d} \approx (1-\alpha)\frac{u_\varphi^2(\varpi)}{G^{1/2}B_z(\varpi)\varpi}. \tag{1.5}$$

Inserting the values of B_z, u_φ, and ϖ measured in OH maser rings around a few high-mass protostars (see Table 1.1), we obtain values of λ_{sys} in the range 2–13. Comparing these values of λ_{sys} to the values $\lambda \approx 2$ typical of protostellar cores, we conclude that the mass-to-flux ratio of circumstellar disks around massive stars is somewhat larger, but not by a large factor, than the mass-to flux ratio of the parent cloud. In other words, the magnetic flux trapped in circumstellar disks around stars of mass $M_* \approx 10\ M_\odot$ is only a factor of a few smaller than the flux that would be trapped in the system under field-freezing. These results, if confirmed, suggest that the solution to the catastrophic magnetic braking problem discussed in Sect. 1.3.1 does not require a strong annihilation of magnetic field in the circumstellar region (by, e.g., reconnection and/or turbulence), but rather a redistribution of the field (by a microscopic or macroscopic process) towards a quasi-force-free configuration. In this respect, it will be very important to obtain the mass-to-flux ratios also in disks around low-mass stars, an endeavor that ALMA will make possible in the near future (see chapter by Vlemmings in this volume).

1.4 Magnetized Accretion Disks

1.4.1 Viscosity and Resistivity

As discussed in the previous section, the RSDs drag a fraction of the magnetic flux from the parent core during the gravitational collapse. Once the accretion has stopped, the magnetized disk will evolve subject to two diffusive processes: viscosity, ν, due to turbulent and magnetic stresses, that produces accretion toward the star and transfer of angular momentum outside; and resistivity, η, due to microscopic

collisions and the magnetorotational instability (MRI; see, e.g., review of Balbus & Hawley 1998), which allows matter to slip across field lines. The MRI is considered responsible for the disk "anomalous" viscosity needed to explain the disks lifetimes of $\sim 10^6$ yr (Haisch et al. 2001; Sicilia-Aguilar et al. 2004). As pointed out by Shu et al. (2007), even in the case of a strong poloidal field, magnetized accretion disks can develop the MRI instability.

In these disks, the dragging of field lines by accretion is balanced by the outward field diffusion only if the ratio $\eta/\nu \sim z_0/\varpi \ll 1$, where z_0 is the vertical half disk thickness and ϖ is the radial cylindrical coordinate (Lubow et al. 1994). This result is at variance with the usual assumption of a magnetic Prandtl number $\nu/\eta \sim 1$ in magnetized disks. Moreover, the magnetic tension due to the poloidal magnetic field threading the disk will produce sub-Keplerian rotation (Shu et al. 2007).

In near field freezing conditions, the accretion flow generates a mean radial field from the mean vertical field. This mean radial field has two important consequences: First, it changes the radial force balance and causes sub-Keplerian rotation of the gas. If one neglects the disk self-gravity and gas pressure, the force balance equation is

$$\varpi\Omega^2 = -\frac{B_z B_\varpi^+}{2\pi\Sigma} + \frac{GM_*}{\varpi^2}, \tag{1.6}$$

where Ω is the rotation rate, Σ is the disk mass surface density, B_z is the component of the magnetic field threading vertically through the disk, and B_ϖ^+ is the radial component of the magnetic field just above the disk that responds to the radial accretion
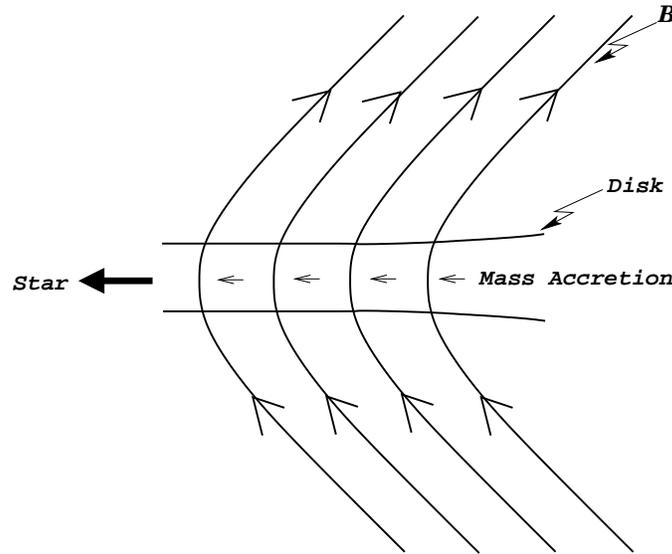

Fig. 1.3 Sketch of magnetized disk where the field lines are dragged by the accretion flow onto the star (from Shu et al. 2007).

flow. The rotation rate, given by the solution of the above equation, is smaller than the Keplerian value $\left(GM_*/\varpi^3\right)^{1/2}$, because of the extra support of the magnetic tension against gravity,

$$\Omega = f\left(\frac{GM_*}{\varpi^3}\right)^{1/2}, \quad \text{with the sub-Keplerian factor } f < 1. \qquad (1.7)$$

Note that the field lines are bent because the sources of the disk magnetization are currents at infinity anchoring magnetic field lines to the parent cloud. Second, the stretching of the poloidal field by differential rotation produces an azimuthal field in the disk that, coupled with the radial field, exerts a mean stress and torques the gas, allowing the disk viscous evolution. In the absence of numerical simulations of the MRI that are both global and have a non-zero net magnetic flux, Shu et al. (2007) proposed a functional form of the viscosity based on mixing length arguments,

$$\nu = D\frac{B_z^2 z_0}{2\pi\Sigma\Omega}, \qquad (1.8)$$

where $D \leq 1$ is a dimensionless coefficient. Since, as discussed above, the resistivity η is related to viscosity in steady state, Shu et al. were able to construct full radial models of disks around young stars. They find that the disk masses, sizes and magnetic field strengths are consistent with the observations. The coefficient D should acquire small values if there are substantial "dead zones", where the ionization is too low to couple to magnetic fields except, possibly, for thin surface layers (as could be the case in disks around T Tauri stars). They propose that rapid transport of mass and magnetic fluctuations across strong mean field lines can occur through the reconnection of small magnetic loops, twisted and bent by the turbulent flow, this process being the source of the disk viscous and resistive diffusivities. Since the microscopic disk resistivities drop at large radii ($\varpi > 10$–20 AU; see, e.g., Sano et al. 2000), Shu et al. conclude that the MRI has to provide the anomalously large value of the resistivity in the outer disk in order to allow accretion to continue to the central star.

For **a** disk model with standard flaring ($z_0 \propto \varpi^{5/4}$) Equation (1.6) can be recast in the form

$$1 - f^2 = \frac{0.5444}{\lambda_{\text{sys}}^2}\left(\frac{M_*}{M_d}\right). \qquad (1.9)$$

For a closed star plus disk system in which infall has ceased, the mass-to-flux ratio λ_{sys} remains constant. Then, since disk accretion decreases the disk mass M_d relative to stellar mass M_*, the departure from Keplerian rotation, $(1 - f^2)$, must grow with time. This happens because viscosity drains mass from the disk onto the star, while resistivity can only cause the redistribution of flux within the disk but cannot change the total flux, making f decrease with time. Thus, the disk becomes more sub-Keplerian and magnetized with time.

1.4.2 Sub-Keplerian Disk Rotation

Accretion disks threaded by a poloidal magnetic field lines as shown in Figure 1.3, bent with respect to the vertical by angles larger than $30°$, are candidates to produce disk winds (Blandford & Payne 1982; for a recent review on disk winds, see, e.g. Pudritz et al. 2007). In fact, in the models of magnetized disks of Shu et al. (2007) this criterion is comfortably satisfied (see their Table 1). Nevertheless, sub-Keplerian rotation of the gas in accretion disks poses a problem to disk wind models. In order to launch winds, sub-Keplerian disk either have to be warm to overcome the potential barrier, or they need a dynamically fast diffusion across the magnetic field lines (Shu et al. 2008).

In the case of thermal launching, given the fractional deviation from Keplerian rotation $f < 1$, the gas needs to climb the local potential barrier in order to be ejected magnetocentrifugally along field lines. Thus, the gas requires a thermal speed

$$c_s^2 \approx \frac{1}{4}(1 - f^2)\frac{GM_*}{\varpi}. \tag{1.10}$$

One can write this condition as a constraint for the gas temperature in terms of the local escape speed, $u_{esc} = \sqrt{2GM_*/\varpi}$,

$$T \approx 1.4 \times 10^6 \left(1 - f^2\right) \left(\frac{u_{\mathrm{esc}}}{200\,\mathrm{km\,s^{-1}}}\right) K. \tag{1.11}$$

Thus, for a deviation from Keplerian rotation as small as $f = 0.95$, typical of protostellar disks, the gas temperature need to be as large as $T \sim 1.4 \times 10^5 K$ to eject a disk wind that can reach typical protostellar speeds of $\sim 200\,\mathrm{km\,s^{-1}}$. Since the disks around young stars are cold ($T < 1000\,K$; e.g., D'Alessio et al. 1999) thermal launching is not a viable mechanism for magnetocentrifugal disk winds.

Resistive launching is in fact used by current disk wind models that use a large resistivities that allow the gas to diffuse vertically across magnetic field lines to the launching point where $f = 1$ (see, e.g., Figure 5 of Ferreira & Pelletier 1995 showing f as a function of height). Nevertheless, fast diffusion also occurs radially, and, as a result, these models have accretion speeds of the order of the sound speed, $u_\varpi \sim c_s$. Such large speeds imply too short accretion timescales

$$\tau_{\mathrm{acc}} = \frac{\varpi}{u_\varpi} \sim 2,400 \left(\frac{\varpi}{100\,\mathrm{AU}}\right) \left(\frac{c_s}{0.2\,\mathrm{km\,s^{-1}}}\right)^{-1} \mathrm{yr}, \tag{1.12}$$

i.e., these models have too short disk lifetimes (see §1.4.1).

Therefore, magnetocentrifugally-driven, cold, disk wind models need to face the challenge imposed by the sub-Keplerian gas rotation due to the support provided by magnetic tension by a dynamically important poloidad field: disk winds cannot be launched thermally and diffusive launching makes the disks short lived.

1.4.3 Stability and Planet Formation

Gravitational instabilities in accretion disks around young stars can grow in the non-linear regime and produce secondary bodies within the disk, such as brown dwarfs and giant planets. On the other hand, if the growing perturbations saturate, the gravitational torques can lead to redistribution of angular momentum and disk accretion. In non magnetic disks, both processes require the onset of gravitational instability, which, for axisymmetric perturbations, is determined by the value of the Toomre parameter Q_T,

$$Q_T \equiv \frac{c_s \kappa}{\pi G \Sigma}, \qquad (1.13)$$

where $\kappa = \varpi^{-1}[\partial(\varpi^2 \Omega)^2/\partial \varpi]^{1/2}$ is the epicyclic frequency (Toomre 1964).

In the presence of magnetic fields, however, the condition of gravitational instability is modified. The modification to the Toomre criterion for a magnetized disk has been discussed previously in the Galactic context by several authors (e.g., see Elmegreen 1994). However the magnetic field in the Galaxy is likely to be dynamo-generated and mostly toroidal (see chapter by Beck, this volume), whereas in a circumstellar disk the magnetic field is expected to be mostly poloidal and dragged from the parent cloud. From a linear stability analysis, Lizano et al. (2010) derived the modified Toomre Q_M parameter for a disk threaded by a poloidal magnetic field, which provides the boundary of stability for axisymmetric ($m = 0$) perturbations, given by

$$Q_M = \frac{\Theta^{1/2} a \kappa}{\pi \varepsilon G \Sigma_0}, \qquad (1.14)$$

where

$$\Theta \equiv 1 + \frac{B_z^2 z_0}{2\pi \Sigma c_s^2} \quad \text{and} \quad \varepsilon \equiv 1 - \frac{1}{\lambda^2}, \qquad (1.15)$$

and $\lambda = 2\pi G^{1/2}\Sigma/B_z$ is the local value of the mass-to-flux ratio in the disk. For $Q_M < 1$, perturbations with wavenumber between $k_\pm = k_{\max}(1 \pm \sqrt{1 - Q_M^2})$ are unstable, with $k_{\max} = (\varepsilon/\Theta)k_J$ being the wavenumber of maximum growth, and $k_J = \pi G \Sigma/c_s^2$ the Jeans wavenumber. Since $\varepsilon/\Theta < 1$, the effect of the magnetic field is to increase the length scale of the gravitational instability with respect to the Jeans length scale.

Another important factor that determines Q_M in Equation (1.14) is the epicyclic frequency. As discussed in §1.4.1, magnetized disks around young stars rotate at sub-Keplerian speeds because magnetic tension modifies the force balance equation, then $\kappa = f\Omega_K$. Therefore, the inclusion of magnetic fields produces competing effects on the instability parameter Q_M: the strong fields enforce sub-Keplerian flow, which reduces Q_M and leads to greater instability; on the other hand, both magnetic pressure and magnetic tension act to increase Q_M and lead to enhanced stability. For typical disks around low- and high-mass stars, the stabilizing effect wins in the inner regions, as shown in Figure 1.4. Thus, stable magnetized disks can be more massive than their non-magnetized counterparts. The two panels in Figure
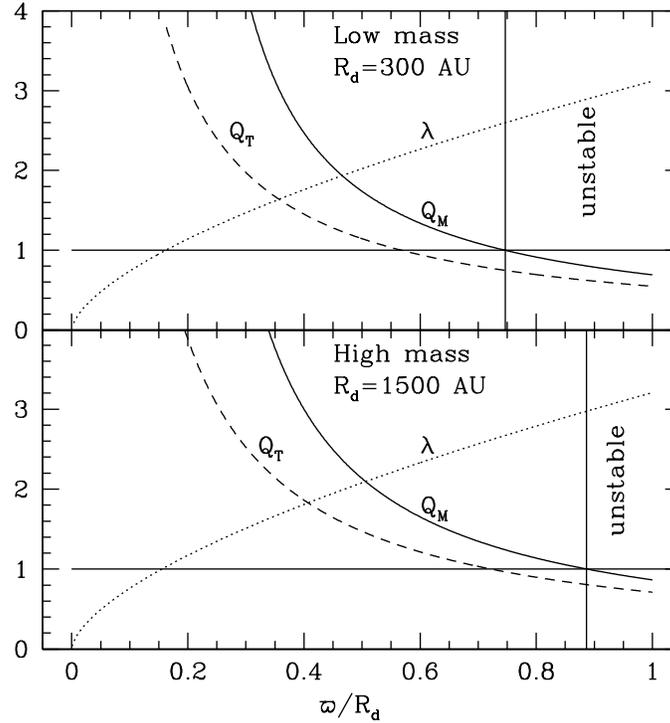
Fig. 1.4 Radial profiles of the Toomre stability parameter Q_T, the magnetic stability parameter Q_M, and the local mass-to-flux ratio λ in typical disks around high-mass stars (lower panel) and low-mass stars (upper panel). These profiles are obtained from the disk models of Shu et al. (2007) with an aspect ratio $\propto \varpi^{1/4}$. The radial coordinate is normalized to the disk radius R_d.

1.4 show the values of the parameters Q_T, Q_M and the local mass-to-flux ratio λ, for the disk models of Shu et al. (2007) as function of the normalized disk radius ϖ/R_d. Since Q_M is always larger than Q_T, the magnetic field has a stabilizing effect against gravity, the radius of the stable region increasing by ~ 20–30% with respect to a nonmagnetic disk. Correspondingly, the fraction of stable enclosed disk mass, $m(\varpi)/M_d$, where M_d is the total disk mass, increases by ~ 30–40%. Also, the unstable region is magnetically supercritical ($\lambda > 1$), as required to allow local gravitational collapse.

The increased stability of magnetized disks against gravitational perturbations poses an obstacle to the formation of giant planets, or somewhat larger secondary bodies such as brown dwarfs, by this process. As discussed by Lizano et al. (2010), the formation of giant planets in the outer parts of disks where $Q_M < q_* \approx 2$ has to satisfy, in addition, the condition of short cooling time $\tau_{\rm cool}$, and the rapid loss of an appreciable amount of magnetic flux. The coupled constraints on Q_M and $\tau_{\rm cool}$ result

in a condition for the Minimum Mass Solar Nebula (MMSN) disk, on the minimum radius outside which giant planet formation can occur,

$$\varpi > 1100 \, (f\mathscr{F})^2 \, \text{AU}, \qquad (1.16)$$

where $\mathscr{F} \approx 0.5$ is a nondimensional quantity that depends on the mass-to-flux ratio λ. The condition on the magnetic flux loss gives a constraint on the disk resistivity

$$\eta > 2.5 \times 10^{18} \, \text{cm}^2 \, \text{s}^{-1}, \qquad (1.17)$$

larger than the microscopic resistivity.

Therefore, magnetic fields stabilize protoplanetary disks, and make it more difficult to form giant planets via gravitational instability. At any rate, this process can occur only at large radii.

1.4.4 Implications of Disk Magnetization for Planet Migration

Protoplanets experience orbital migration due to angular momentum exchange by tidal interactions with the disk material. There are several types of tidal interactions that occur through wave excitation or advected disk material: Type I migration applies to embedded protoplanets; Type II migration occurs when the protoplanet is massive enough to open a gap; and Type III migration is driven by coorbital torques (see review Papaloizou & Terquem 2006). In magnetized disks, sub-Keplerian rotation results in a new migration mechanism for embedded proto-planets (Adams et al. 2009). These bodies rotating at Keplerian speed, $\Omega_K = (GM_*/r^3)^{1/2}$, where r is the planet semi-major axis, experience a headwind against the magnetically controlled gas that rotates at sub-Keplerian speeds. The drag force drives their inward migration. The relative speed between the gas and the proto-planet is $u_{\text{rel}} = (1-f)\Omega_K r$, and the torque is

$$T = C_D \pi R_P^2 r \rho_g u_{\text{rel}}^2 = \frac{\pi}{2} C_D (1-f)^2 \, \Omega_K^2 r^3 R_P^2 \left(\frac{\Sigma}{z_0} \right), \qquad (1.18)$$

where $C_D \sim 1$ is the drag coefficient, R_P is the planet radius, $\rho_g = \Sigma/2z_0$ is the gas density, and z_0 is the disk scale height. Assuming circular orbits, the time change of the planet's angular momentum gives the time evolution of r

$$\frac{1}{r}\frac{dr}{dt} = \frac{2T}{m_P \Omega_K r^2}, \qquad (1.19)$$

that implies a migration timescale $t_M \sim 70,000$ yr for an Earth-like planet in a MMSN disk with $f \sim 0.66$.

This mechanism dominates over Type I migration for sufficiently small planets with masses $m_P \leq 1M_{\text{Earth}}$, and/or close orbits $r < 1$ AU. Taking into account both mechanisms, the total migration time t_M moderately decreases due to
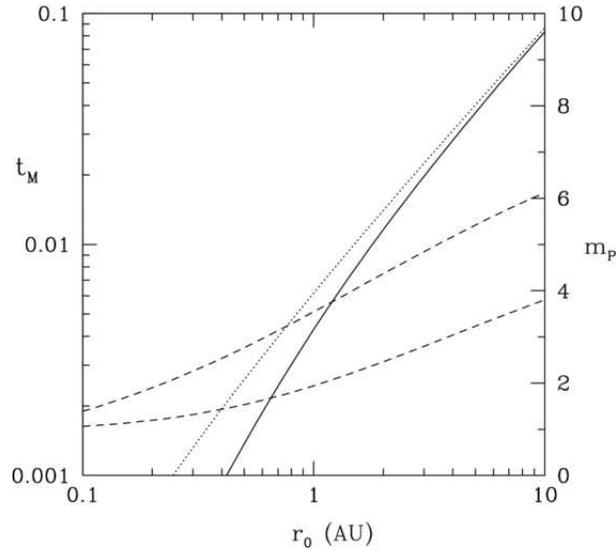
Fig. 1.5 Migration time and final core mass versus starting radius, r_0. The solid curve shows migration time t_M in Myr (left axis) including sub-Keplerian and Type I torques. The dotted curve shows t_M for Type I torques only. The dashed curves show final core mass m_P in M_x (right axis) for migration with both torques (bottom) and Type I torques only (top) (from Adams et al. 2009).

the sub-Keplerian torques, but the mass accreted by planetary cores during the migration epoch changes more substantially, as shown in Figure 1.5. Furthermore, Paardekooper (2009) showed that disk-planet interactions in Type I migration are affected by the degree of disk sub-Keplerian rotation because the position of the Linblad and corotation resonances change with the sub-Keplerian factor f. Paardekooper concluded that migration in sub-Keplerian disks, in general, will be directed inwards and will be sped up compared to Keplerian disks. In general, Type I migration is very fast, with timescales of the order of 10^5 yr, implying that low-mass planets have a hard time surviving in gaseous disks; thus, they would need to form at later times, when the gas has been accreted or dispersed. Moreover, as discussed by Papaloizou & Terquem (2006), even the survival of the rocky cores of giant planets would be compromised unless this type of migration is somehow suppressed or modified by, for example, eccentricity effects (Papaloizou 2002), large scale toroidal magnetic fields (Terquem 2003), stocastic torques due to the presence of turbulence (Nelson and Papaloizou 2004; Laughlin et al. 2004; Adams & Bloch 2009); or by disk opacity effects (Menou & Goodman 2004; Paardekooper & Mellema 2006).

1.5 Conclusions

Magnetic fields are dynamically important for star formation. The measured levels of cloud magnetization, $\lambda = 1$–4, imply that the clouds are close to the critical value of the mass-to-flux ratio to provide support against gravitational collapse. Also, observations of polarized dust emission and statistical analysis of polarization maps strongly suggest that the field is well ordered on pc scales, and has only a relatively small turbulent component.

Although it has been believed since the 1970s that magnetic braking is responsible for the loss of angular momentum in cloud cores, an unexpected result has been the theoretical finding that in an ideal MHD flow the magnetic braking becomes so efficient as to prevent the formation of centrifugally supported disks. Therefore, magnetic field diffusion and/or dissipation in the high density regime of gravitational collapse is needed to avoid catastrophic braking. Field dissipation was also advocated to solve the magnetic flux problem in newly born stars. Several non ideal MHD diffusion processes, able to redistribute the magnetic field brought by gravity in the collapse region, have been studied in analytic and numerical simulations to alleviate the catastrophic magnetic braking, but all of them have been found relatively inefficient. Thus, at the moment, the problem has not yet been resolved. Conversely, solutions based on magnetic reconnection may require high levels of turbulence, which are generally not observed in dense cloud cores.

Once the centrifugally supported disks form, they are expected to have important levels of magnetization due to the incomplete diffusion and /or dissipation of the magnetic field dragged during the gravitational collapse. The strong poloidal field produces sub-Keplerian rotation of the gas because magnetic tension provides support against gravity. This slower rotation poses a local potential barrier that disk winds have to overcome, either by thermal pressure or by fast diffusivity, to reach the launching point where magnetocentrifugal acceleration can take place. Since thermal launching is not possible in cold disks around low-mass stars, disk wind models rely on fast diffusion of the gas across field lines. However, this fast diffusion also produces accretion flows with velocities of the order of the sound speed, that will empty the disk into the star in very short timescales, of only several thousand years. Up to now, no solution has been proposed to this conundrum. Sub-Keplerian rotation of the gas in the disk also produces a headwind on forming proto-planets that move at Keplerian speeds, making them lose angular momentum and migrate faster toward the central star.

Finally, the magnetic fields modify the disk stability by two opposing effects: magnetic pressure and tension support the gas against gravitational collapse, but sub-Keplerian rotation makes the gas locally more unstable. The resulting magnetically modified Toomre stability parameter, Q_M, is in general larger than its non-magnetic counterpart in accretion disks around young stars. Thus, stable magnetized disks can be more massive that nonmagnetic disks. The region of instability is pushed at larger radii, making it more difficult to form giant planets via gravitational instability.

In the near future, ALMA will be able to measure magnetic fields and disk rotation curves with unprecedented spatial resolution and test the theoretical models discussed here. BLAST-pol will map the magnetic field direction of a large sample of molecular clouds and determine the relative strength of the large scale versus the turbulent magnetic field components testing the importance of magnetic fields in cloud support and evolution.

References

1. Adams, F. C., & Bloch, A. M. 2009, ApJ, 701, 1381
2. Adams, F. C., Cai, M. J., & Lizano, S. 2009, ApJL, 702, L182
3. Adams, F. C., & Shu, F. H. 2007, ApJ, 671, 497
4. Allen, A., Shu, F. H., & Li, Z.-Y. 2003, ApJ, 599, 351
5. Armitage, P. J. 2011, ARAA, 49, 195
6. Balbus, S. A., & Hawley, J. F. 1998, Rev. Mod. Phys., 70, 1
7. Ballesteros-Paredes, J., Hartmann, L. W., Vázquez-Semadeni, E., Heitsch, F., & Zamora-Avilés, M. A. 2011a, MNRAS, 411, 65
8. Ballesteros-Paredes, J., Vázquez-Semadeni, E., Gazol, A., et al. 2011b, MNRAS, 416, 1436
9. Blandford, R. D., & Payne, D. G. 1982, MNRAS, 199, 883
10. Braiding, C. R., & Wardle, M. 2012, MNRAS, 422, 261
11. Caselli, P., Walmsley, C. M., Terzieva, R., & Herbst, E. 1998, ApJ, 499, 234
12. Cesaroni, R., Galli, D., Lodato, G., Walmsley, C. M., & Zhang, Q. 2007, Protostars and Planets V, 197
13. Chandrasekhar, S., & Fermi, E. 1953, ApJ, 118, 113
14. Commerçon, B., Hennebelle, P., & Henning, T. 2011, ApJL, 742, L9
15. Crutcher, R. M., & Troland, T. H. 2008, ApJ, 685, 281
16. Crutcher, R. M. 2012, ARAA, 50, 29
17. D'Alessio, P., Calvet, N., Hartmann, L., Lizano, S., & Cantó, J. 1999, ApJ, 527, 893
18. Dapp, W. B., & Basu, S. 2010, A&A, 521, L56
19. Dapp, W. B., Basu, S., & Kunz, M. W. 2012, A&A, 541, A35
20. Duffin, D. F., & Pudritz, R. E. 2009, ApJL, 706, L46
21. Edris, K. A., Fuller, G. A., & Cohen, R. J. 2007, A&A, 46, 865
22. Elmegreen, B. G. 1994, ApJ, 433, 39
23. Falgarone, E., Troland, T. H., Crutcher, R. M., & Paubert, G. 2008, A&A, 487, 247
24. Ferreira, J., & Pelletier, G. 1995, A&A, 295, 807
25. Fromang, S., Hennebelle, P., & Teyssier, R. 2006, A&A, 457, 371
26. Galli, D., Cai, M., Lizano, S., & Shu, F. H. 2009, RevMxAA(SC), 36, 143
27. Galli, D., Lizano, S., Shu, F. H., & Allen, A. 2006, ApJ, 647, 374
28. Galli, D., & Shu, F. H. 1993a, ApJ, 417, 220
29. Galli, D., & Shu, F. H. 1993b, ApJ, 417, 243
30. Glassgold, A. E., Galli, D., & Padovani, M. 2012, ApJ, 756, 157
31. Goldsmith, P. F., Heyer, M., Narayanan, G., et al. 2008, ApJ, 680, 428
32. Girart, J. M., Beltrán, M. T., Zhang, Q., Rao, R., & Estalella, R. 2009, Science, 324, 1408
33. Girart, J. M., Rao, R., & Marrone, D. P. 2006, Science, 313, 812

34. Gonçalves, J., Galli, D., & Girart, J. M. 2008, A&A, 490,2008
35. Haisch, K. E., Jr., Lada, E. A., & Lada, C. J. 2001, ApJL, 553, L153
36. Hennebelle, P., & Ciardi, A. 2009, A&A, 506, L29
37. Hennebelle, P., & Fromang, S. 2008, A&A, 477, 9
38. Hennebelle, P., & Teyssier, R. 2008, A&A, 477, 25
39. Hildebrand, R. H., Kirby, L., Dotson, J. L., Houde, M., & Vaillancourt, J. E. 2009, ApJ, 696, 567
40. Hosking, J. G., & Whitworth, A. P. 2004, MNRAS, 347, 3
41. Houde, M., Vaillancourt, J. E., Hildebrand, R. H., Chitsazzadeh, S., & Kirby, L. 2009, ApJ, 706, 1504
42. Hutawarakorn, B., & Cohen, R. J. 1999, MNRAS, 303, 845
43. Hutawarakorn, B., & Cohen, R. J. 2005, MNRAS, 357, 338
44. Hutawarakorn, B., Cohen, R. J., & Brebner, G. C. 2002, MNRAS, 330, 349
45. Johns-Krull, C. M., Valenti, J., & Koresko, C. 1999, ApJ, 516, 900
46. Johns-Krull, C. M., Valenti, J. A., & Saar, S. H. 2004, ApJ, 617, 1204
47. Joos, M., Hennebelle, P., & Ciardi, A. 2012, arXiv:1203.1193
48. Klessen, R. S., Ballesteros-Paredes, J., Vázquez-Semadeni, E., & Durán-Rojas, C. 2005, ApJ, 620, 786
49. Königl, A., & Salmeron, R. 2011, Physical Processes in Circumstellar Disks around Young Stars, University of Chicago Press, ed. Paulo J. V. Garcia, 283
50. Krasnopolsky, R., & Königl, A. 2002, ApJ, 580, 987
51. Krasnopolsky, R., Li, Z.-Y., & Shang, H. 2010, ApJ, 716, 1541
52. Krasnopolsky, R., Li, Z.-Y., & Shang, H. 2011, ApJ, 733, 54
53. Krumholz, M. R., Crutcher, R. M., & Hull, C. L. H. 2013, ApJL, 767, L11
54. Laughlin, G., Steinacker, A., & Adams, F. C. 2004, ApJ, 608, 489
55. Lazarian, A., & Vishniac, E. T. 1999, ApJ, 517, 700
56. Li, Z.-Y., & Shu, F. H. 1996, ApJ, 472, 211
57. Li, Z.-Y., Krasnopolsky, R., & Shang, H. 2011, ApJ, 738, 180
58. Li, Z.-Y., Krasnopolsky, R., & Shang, H. 2013, arXiv:1301.6545
59. Lizano, S., Galli, D., Cai, M. J., & Adams, F. C. 2010, ApJ, 724, 1561
60. Lizano, S. & Shu, F. 1989, ApJ, 342, 834
61. Lubow, S. H., Papaloizou, J. C. B., & Pringle, J. E. 1994, MNRAS, 267, 235
62. Machida, M. N., Inutsuka, S.-I., & Matsumoto, T. 2011, PASJ, 63, 555
63. Mellon, R. R., & Li, Z.-Y. 2008, ApJ, 681, 1356
64. Mellon, R. R., & Li, Z.-Y. 2009, ApJ, 698, 922
65. Menou, K., & Goodman, J. 2004, ApJ, 606, 520
66. Mestel, L., & Spitzer, L. 1956, MNRAS, 116, 503
67. Mouschovias, T. C., & Ciolek, G. E. 1999, NATO ASIC Proc. 540: The Origin of Stars and Planetary Systems, 305
68. Nakamura, F., & Li, Z.-Y. 2008, ApJ, 687, 354
69. Nakano, T. 1979, PASJ, 31, 697
70. Nakano, T., Nishi, R., & Umebayashi, T. 2002, ApJ, 573, 199
71. Nelson, R. P., & Papaloizou, J. C. B. 2004, MNRAS, 350, 849
72. Paardekooper, S.-J. 2009, A&A, 506, L9
73. Paardekooper, S.-J., & Mellema, G. 2006, A&A, 459, L17
74. Padoan, P., Juvela, M., Goodman, A. A., & Nordlund, Å. 2001, ApJ, 553, 227
75. Padovani, M., Galli, D., & Glassgold, A. E. 2009, A&A, 501, 619
76. Papaloizou, J. C. B. 2002, A&A, 388, 615
77. Papaloizou, J. C. B., & Terquem, C. 2006, Reports on Progress in Physics, 69, 119
78. Pineda, J. E., Goodman, A. A., Arce, H. G., et al. 2010, ApJL, 712, L116
79. Pinto, C., & Galli, D. 2008, A&A, 484, 17
80. Pinto, C., Galli, D., & Bacciotti, F. 2008, A&A, 484, 1
81. Price, D. J., & Bate, M. R. 2007, MNRAS, 377, 77
82. Pudritz, R. E., Ouyed, R., Fendt, C., & Brandenburg, A. 2007, Protostars and Planets V, 277
83. Santos-Lima, R., de Gouveia Dal Pino, E. M., & Lazarian, A. 2012, ApJ, 747, 21

84. Santos-Lima, R., de Gouveia Dal Pino, E. M., & Lazarian, A. 2013, MNRAS, 429, 3371
85. Seifried, D., Banerjee, R., Klessen, R. S., Duffin, D., & Pudritz, R. E. 2011, MNRAS, 417, 1054
86. Seifried, D., Banerjee, R., Pudritz, R. E., & Klessen, R. S. 2012, MNRAS, 423, L40
87. Sano, T., Miyama, S. M., Umebayashi, T., & Nakano, T. 2000, ApJ, 543, 486
88. Shu, F. H., Galli, D., Lizano, S., & Cai, M. J. 2006, ApJ, 647, 382
89. Shu, F. H., Galli, D., Lizano, S., Glassgold, A. E., & Diamond, P. H. 2007, ApJ, 665, 535
90. Shu, F. H., Lizano, S., Galli, D., Cai, M. J., & Mohanty, S. 2008, ApJ, 682, L121
91. Sicilia-Aguilar, A., Hartmann, L. W., Briceño, C., Muzerolle, J., & Calvet, N. 2004, AJ, 128, 805
92. Tang, Y.-W., Ho, P. T. P., Koch, P. M., Girart, J. M., Lai, S.-P., & Rao, R. 2009, ApJ, 700, 251
93. Terquem, C. E. J. M. L. J. 2003, MNRAS, 341, 1157
94. Toomre, A. 1964, ApJ, 139, 1217
95. Tomisaka, K. 2002, ApJ, 575, 306
96. Tomisaka, K., Ikeuchi, S., & Nakamura, T. 1990, ApJ, 362, 202
97. Vázquez-Semadeni, E., Kim, J., Shadmehri, M., & Ballesteros-Paredes, J. 2005, ApJ, 618, 344